Investigation of SAR Reduction Using Flexible Antenna with Metamaterial Structure in Wireless Body Area Network

Mengjun Wang, Ze Yang, Jianfei Wu, Jianhui Bao, Jianying Liu, Lulu Cai, Tao Dang, Hongxing Zheng, *Member, IEEE*, Erping Li, *Fellow, IEEE*

***Abstract*— A flexible dual-band antenna with a metamaterial structure is presented. Polyimide substance, which makes the antenna thin and bendable, is used as the substrate for the antenna. When the metamaterial structure is placed between the antenna and the human's forearm, the antenna gain is increased by 9.3 dB and 5.37 dB, and the radiation efficiency is increased by 48.4% and 35.7%, at 2.45 and 5.8 GHz, respectively. In addition, the specific absorption rate (SAR) is decreased by more than 70%, considering the limitations imposed by Federal Communications Commission and the regulation of International Commission on Non-Ionizing Radiation Protection (ICNIRP) for the frequencies cited above. The fabricated prototype of the antenna with the integrated metamaterial structure was investigated by placing it on different places of human body, as also on different human bodies. The obtained results show that the proposed antenna is safe and suitable for use, in terms of the ICNIRP standards of World Health Organization.**

***Index Terms*—Specific absorption rate, flexible antenna, wireless body area network, metamaterial structure, artificial magnetic conductor.**

I. Introduction

WIRELESS body area network (WBAN), a body-centric wireless communication system, is used for monitoring human body's health condition. The system collects and transmits useful data to the hospital or data analysis centre [1], and antenna plays an important role in transmitting/receiving signals. The antenna can be put on the human body, together with the terminal device [2], or even embedded into the body [3]. In their quest for providing a good communication service to the WBAN system, the researchers have recently found that flexible antenna meets the requirements best. This is because most antennas used in traditional communication systems are rigid and hence create an uncomfortable feeling, when placed on the human body; besides, handling rigid antennas is inconvenient. To overcome these problems, some earlier workers suggested soft materials such as polyimide [4], polycarbonate [5] and polyethylene [6] as the substrate for antennas. These materials are flexible and robust, with good thermal endurance.

Of late, flexible antenna, based on soft substrates, has become a hot research topic. Antennas become bendable when their substrates are clad by thin copper film. Earlier, the flexible antenna was fabricated on the textile material [7], but it did not work, because it does not really touch the human body. Later, other soft materials, such as natural rubber, were used by Alias et al [8] in designing a microstrip patch antenna. Different carbon fillers were added to the rubber to improve the substrates' mechanical and electrical properties. However, the performance of antennas with rubber substrates, in terms of their robustness and thermal endurance, was found to be unsatisfactory. Cook et al [9] used paper as the bendable substrate, by virtue of its low cost, ease of fabrication, and organic nature. Even this was found to be of no use, particularly for outdoor applications. Against this backdrop, polyimide emerged as the natural choice for the substrate material to the present authors for designing a flexible antenna.

In general, electromagnetic wave radiation is highly harmful to human health. Besides, when the antenna is close to the human body, it is affected by human body's biological organization. To mitigate the harmful effects of radiation from the antenna, an artificial magnetic conductor (AMC) has been proposed as a support for the antenna, which can reflect most of the electromagnetic wave energy in some frequencies. A dual-band planar array was designed, with 3.048 mm thickness, [10], by creating an annular slot in a square patch, in each array unit. It was then found that the antenna gain increased by almost 10 dB; besides, the front-to-back ratio was 15 dB. However, the antenna was rather thick. A dual-band coplanar patch textile antenna, with a square fabric electromagnetic band gap structure, was proposed [11], which can be patched onto the human body as a body-warning system. Then a 3×3 element

Manuscript received March 9, 2017; revised January 11, 2018 and March 14, 2018; accepted March 19, 2013. Date of publication xxx xx, 2018. This work is supported by the High-level Personal Research Projects of Higher Education Schools in Hebei Province (No. GCC2014011), 2015 Foreign Experts Affairs Talents Introduce Projects in Hebei Province, and 2017 Innovation Funding Project of Postgraduate in Hebei Province (No. CXZZSS2017034), China. It is also supported, in part, by the National Natural Science Foundation of China, under Grant 61671200, 61371031, 61571395, and by the open project of Zhejiang Key Lab. for Advanced Microelectronic Intelligent Systems and Applications (ZJUAMIS1703).

M. Wang, Ze. Yang, J. Bao, J. Liu, L. Cai, and H. Zheng are with the School of Electronics and Information Engineering, Hebei University of Technology, Tianjin 300401, China (e-mail: wangmengjun@hebut.edu.cn; hxzheng@hebut.edu.cn).

J. Wu was with the School of Information and Communication Engineering, National University of Defense Technology, Changsha 410073, China. He is now with the Tianjin Binhai Civil-military Integrated Innovation Institute, Tianjin 300450, China (e-mail: wujianfei990243@126.com).

T. Dang is with Generic Technology Research Department, Sichuan Jiuzhou Electronic Technology Co., Ltd, Mianyang, Sichuan 621000, China (e-mail: dangtao jiuzhou@126.com).

E. Li is with the Department of Electronic Engineering, Zhejiang University, Hangzhou 310007, China. (e-mail: liep@zju.edu.cn).

This article has been accepted for publication in a future issue of this journal, but has not been fully edited. Content may change prior to final publication. Citation information: DOI 10.1109/TAP.2018.2820733, IEEE Transactions on Antennas and Propagation

array was designed, which can reduce the radiation energy entering the body by over 10 dB, and improve the antenna gain by 3 dB. This renders integration of the dual band antenna with band gap surface possible, and the device so integrated was found to work very well, when placed on the human body. However, even those antennas were too big and thick to fit into the WBAN applications. Therefore, the focus of research shifted to smaller and thinner designs. A flexible dual-band antenna was designed, with 1.7 mm thick AMC structure [12] but, its data, in terms of specific absorption rate (SAR), as defined by the World Health Organization [13], was not verified prior to integrating the antenna with the AMC. An M-shaped printed monopole antenna, with a slot Jerusalem Cross AMC, was investigated [14]. Although the experimental results show improvement in radiation, impedance matching, and SAR, as compared to conventional monopole and dipole antennas, no verification data was obtained from that antenna. To guarantee the safety of WBAN system, it should be ensured that SAR values and electromagnetic radiation are under control.

In this study, a flexible antenna with metamaterial structure (MS) was designed and investigated to ascertain its usefulness and safety. The newly designed antenna with MS is thinner than the earlier models; besides, its SAR decreased considerably. It also eliminates frequency offset, besides achieving increase in the antenna gain. Fabricated samples of the antenna, integrated with MS, were tested by studying their radiation patterns when the antenna was placed on different places of the human body, and on different human bodies.

The remainder of this paper is organized as follows: Section II presents a detailed description of the antenna design, for which Computer Simulation Technology (CST) and Microwave Studio software [15] were used in analyzing the antenna's size and electric properties; Section III deals with implementation of the experiment and checking the properties of the antenna, integrated with MS; Section IV analyzes the radiation patterns obtained by placing the proposed structure on different parts of the human body; finally, Section V sums up the conclusions drawn from this study.

II. Design of Antenna and Metamaterial Structure

A. Demission and Size Design

For investigating the dual-band antenna, with bendable properties, brunching technique was used, and thin copper film selected as the polyimide substrate. The fabricated antenna has two branches, forming a U-shaped radiating element, as shown in Fig. 1. Straight strip line is replaced by fold line on the top of radiator to obtain compactness in size. Then the closed strip loop was cut apart leaving an open symmetrical gap 'm' in the middle of the radiator, which leads to multi-modes, which is characteristic of the antenna. Dual-band operation was achieved by adjusting the fold and the size of 'm'. At the bottom of the substrate, a coplanar waveguide (CPW) transmission line, with a signal strip of width $W_1$and two gaps of g, excites the radiator. Two rectangular patches support the antenna in the ground plane. The CPW feed technique can reduce the fabrication complexity of the antenna, because both the radiator and the ground plane are located on the same side of the substrate.

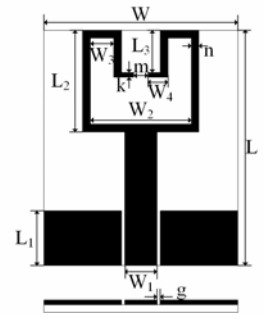

Fig. 1. Geometry of the proposed antenna, fed by the CPW; the optimized size parameters are shown in Table I.

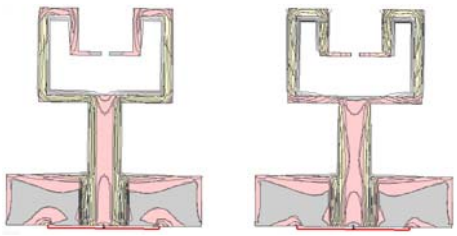

(a) (b)

Fig. 2. Current distribution in the designed antenna; these results were obtained by using the CST simulation at (a) 2.45 GHz and (b) 5.8 GHz.

Polyimide of 50 μm thickness, with dielectric constant ε_r=3.5 and loss tangent δ=0.027, was used as the flexible substrate, on which a 35μm thick coated copper film was placed. To obtain 50Ω characteristic impedance, the sizes of W_1, g and L_1, and other dimensions must be investigated carefully.

The antenna was designed to operate at 2.45 GHz and 5.8 GHz frequencies. Current distribution in this antenna, obtained by using CST simulator, is shown in Fig. 2. From Fig. 2 (a), it can be seen that the current density is higher at the bottom of the U-shaped strip and transmission line than at other places. This indicates that the frequency f_1=2.45 GHz was produced by one wavelength approximately. Fig. 2 (b) shows that the current distribution is more intensive (5.8 GHz) at the top of the U-shaped strip and transmission line. This implies that the frequency f_2=5.8 GHz was generated by two wavelengths, and this size is nearer to the length of U-shaped strip. The other dimensions of the antenna design can be obtained by the following theoretical analysis.

The effective dielectric constant ε_{eff} of the antenna can be calculated thus:

$$\varepsilon_{eff} = \frac{\varepsilon_r + 1}{2} + \frac{\varepsilon_r - 1}{2}\left(1 + 12\frac{h}{W_1}\right)^{-1/2} . \quad (1)$$

Substitution of polyimide substrate dimensions ε_r=3.5, h=50μm, and W_1=4mm into equation (1) gives that ε_{eff}=3.42. f_1 and f_2 can be expressed approximately as follows:

$$f_{1,2} = \frac{c}{\sqrt{\varepsilon_{eff}} \cdot \lambda_{1,2}} , \quad (2)$$

where λ_1 and λ_2 are the guide wavelengths, c is the velocity of light, and f_1 and f_2 are the resonant frequencies [16].

This article has been accepted for publication in a future issue of this journal, but has not been fully edited. Content may change prior to final publication. Citation information: DOI 10.1109/TAP.2018.2820733, IEEE Transactions on Antennas and Propagation

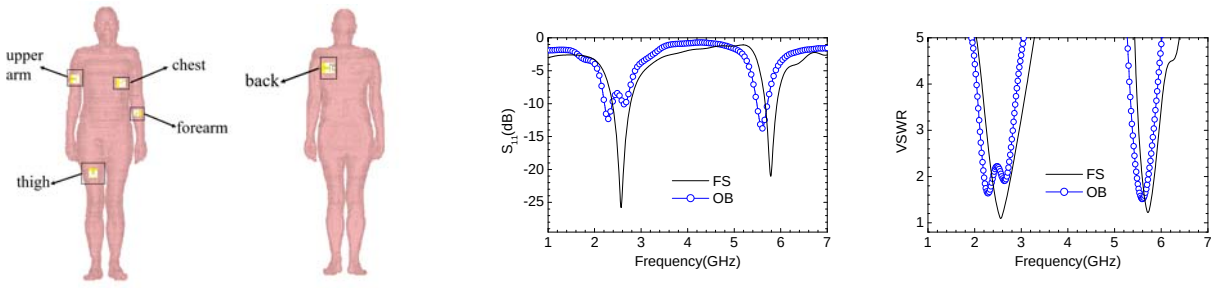

(a) (b) (c)

Fig. 3. Simulated results obtained by placing the antenna on the human body model, Gustav, and using CST software are compared to the results obtained without Gustav. (a) Antenna positions on the forearm, upper arm, thigh, chest and back of the model. (b) Reflection coefficient S_{11} and (c) VSWR, with and without Gustav model, when the antenna was on the forearm. Curves OB and FS refer, respectively, to the results obtained when the antenna was put on the forearm of the Gustav model and in the middle of the simulation area.

From equation (2), the length l of the proposed U-shaped strip can be found out. Obviously, f_1 =2.45 GHz and f_2 =5.8 GHz are related to $\lambda_1 \approx l$ and $\lambda_2 \approx 0.5l$, respectively. Hence, the proposed antenna can be regarded as a two-part radiator of a U-shaped strip, shown in Fig. 2. One part radiates f_1 mode, and the other the f_2 mode. Then, the current path, length of radiator, is expressed approximately by

$$l = W_2 + 2\times L_2 + 2\times W_3 + 2\times L_3 + 2\times W_4 \quad . \tag{3}$$

Other dimensions in this equation can be obtained from numerical experiment by using the CST simulator. The optimized sizes are listed in Table I.

TABLE I. ANTENNA SIZE DIMENSIONS USING CST SIMULATOR (UNIT: MM)

Dimension	L	L_1	L_2	L_3	m	g
Size	30.0	7.0	13.0	5.5	1.0	0.15
Dimension	W	W_1	W_2	W_3	n	k
Size	25.0	4.0	15.0	3.0	1.0	0.5

B. Impact from Human Body

Since the antenna was designed to serve the WBAN system, its performance must be evaluated when it is close to the human body, because human body absorbs/reflects part of the electromagnetic energy. The CST software has a human body model Gustav, which is shown in Fig. 3(a). To speed up computation, the arm's tissue of this model was simplified into four layers for simulation: skin, fat, muscle and bone. As the distance between skin and antenna [17] is crucial to ensure that the proposed antenna works effectively, it is maintained at a distance (d) of 5 mm, i.e., d = 5mm.

The simulated results obtained for reflection coefficient S_{11}, with and without Gustav, are shown in Fig. 3 (b), wherein the curves OB and FS refer respectively to the results obtained when the antenna was put on the Gustav model and in the middle of the simulation area. This holds good for all the figures in this paper. Two operating frequencies are obvious from this figure. When the antenna was put at distance d on the Gustav, its operating frequency changed from 2.6 GHz and 5.8 GHz to 2.2 GHz and 5.6 GHz, respectively. This is because the dielectric constant of human body tissues is higher than that of the polyimide substrate. Voltage Standing Wave Ratio (VSWR) of the antenna is shown in Fig.3(c). Other electric properties, such as gain and radiation pattern also changed and the same were checked carefully.

The radiation pattern of the designed antenna is shown in Fig. 4. In comparison with the radiation patterns in the middle of simulation area, those in other areas are greatly influenced by the human body model. The decrease in radiation in the E-plane and H-plane, and back lobe can be explained as due to human body's effect. Comparative performances of antenna in terms of radiation between air and on human model are presented in Table II, in detail. When the antenna was close to the human body, radiation decreased; simultaneously the gain also decreased at 2.45 GHz because of resonant frequency of the water molecules of human body tissue near this numerical value; it is also observed that some electromagnetic energy has been absorbed. However, the gain increased at 5.8 GHz because of increase in electrical conductivity of body tissue at higher frequency. The frequency (5.8 GHz) is far away resonant frequency of water molecules (2.5GHz). Hence, human body absorbed less electromagnetic energy and reflected more energy.

To protect human body from the effects of harmful radiation, regulatory restrictions are imposed by International Commission on Non-Ionizing Radiation Protection (ICNIRP). As per these regulations, the maximum SAR must not exceed 2.0 W/kg for 10g of tissue. Meanwhile, the Federal Communications Commission (FCC) stipulated that the SAR must not be more than 1.6 W/kg for 1g of tissue. Before using the antenna in WBAN, the SAR must be determined to ensure that it is within the safety limits. Fig. 5 shows the distribution of SAR values in 1g and 10g of inside body tissue at 2.45 GHz and 5.8 GHz. The input power for antenna was 0.5 W, as per IEEE/IEC 62704-1 standard. Table III presents the maximum values of SAR for 1g, and 10g inside body tissues at 2.45 GHz and 5.8 GHz. From this Table, it can be seen that 1g body tissues absorbed much more electromagnetic energy than did the 10g body tissues, and that the human body was exposed to more electromagnetic energy at 2.45 GHz than at 5.8 GHz, because the conductivity of body tissue at 5.8 GHz is higher than that at 2.45 GHz. It can also be seen that the maximum SAR is 17.50 W/kg for averaged 1g body tissue at 2.45 GHz. The experimental results do not obviously satisfy the existing regulations, when the antenna was close to the human body. Therefore, additional measures have to be taken, as explained below, to reduce the SAR to the safety standard level.

This article has been accepted for publication in a future issue of this journal, but has not been fully edited. Content may change prior to final publication. Citation information: DOI 10.1109/TAP.2018.2820733, IEEE Transactions on Antennas and Propagation

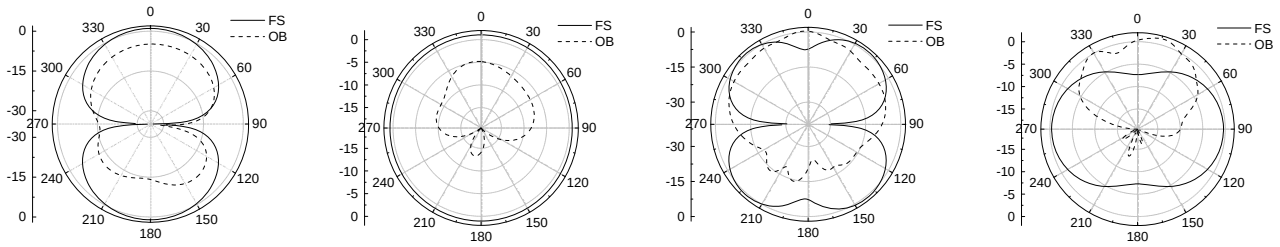

Fig. 4. Comparison of the radiation patterns obtained at 2.4 GHz by placing the antenna (a) on the forearm of Gustav model and (b) in the middle of the simulation area, and those obtained at 5.8 GHz: (c) and (d). E-plane in (a) and (c), H-plane in (b) and (d).

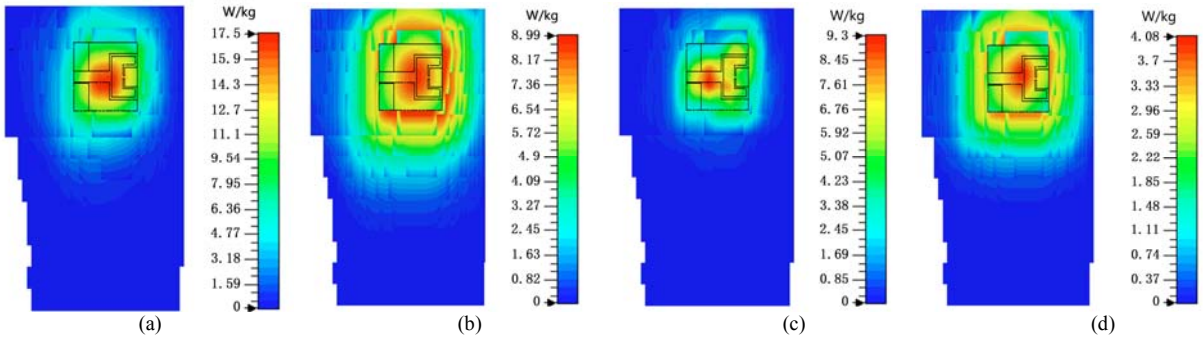

Fig. 5. The SAR values distribution at 2.45 GHz on (a) and (b), and at 5.8 GHz on (c) and (d); (a) & (c) refer to1g of tissue, and (b) & (d) to10g of tissue.

TABLE II. THE PERFORMANCE COMPARISON OF ANTENNA IN FREE SPACE AND ON HUMAN BODY'S FOREARM

Frequency (GHz)	Radiation Efficiency (%)		Gain(dB)	
	Free space	On body	Free space	On body
2.45	82.3	12.9	1.25	-4.1
5.80	82.4	31.5	1.66	2.33

TABLE III. SIMULATED SAR VALUES ON HUMAN BODY (UNIT: W/KG)

Frequency(GHz)	1g	10g
2.45	17.50	8.99
5.80	9.3	4.08

C. *Metamaterial Structure Consideration*

To reduce high SAR values, a metamaterial structure, which can reflect electromagnetic wave in some specific frequency bands, was considered. One element geometry of this structure is depicted in Fig. 6. It consists of three layers: (i) a square metal ring around (ii) a square metal patch on the dielectric substrate, and (iii) another metal layer as the ground plane at the bottom of the substrate. The thickness of the substrate is h; the other dimensions are shown in Fig. 6. Circuit model of this structure is shown in Fig.7, by using the transmission line theory. The metal ring has small series inductance L_1, which can be ignored when compared to the series surface capacitance C_1, caused by the gap between the patch and the ring [18]. Also, the inner metallic patch has small series inductance L_2, which can be ignored, when compared to the series surface capacitance C_2, caused by the gap between the inner patch and the outside ring. The layers between the square patch and the ground plane form capacitance C_h, and the ground plane can be

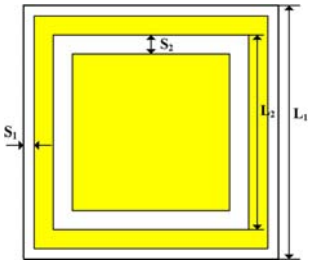

Fig. 6. One element geometry of square metamaterial structure.

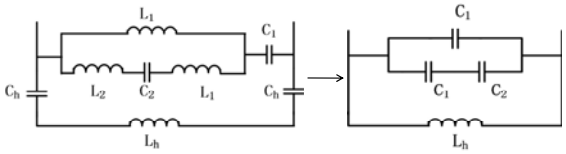

Fig. 7. Equivalent circuit model of the metamaterial structure unit.

modeled as inductance L_h. A more simplified parallel LC resonant circuit also can be achieved by ignoring the small capacitor C_h and the inductances L_1, L_2. As the structure has dual-band properties, it can be divided into lower and higher bands in the equivalent circuit model [19].

For the lower and higher frequency bands, the surface impedances Z_L and Z_H are expressed as follows:

$$Z_L = \frac{1}{j\omega C + \frac{1}{j\omega L_h}} = \frac{j\omega L_h}{1-\omega^2 L_h C} = \frac{j\omega L_h}{1-\left(\omega/\omega_L\right)^2}, \quad (4)$$

$$Z_H = \frac{1}{j\omega C_1 + \frac{1}{j\omega L_h}} = \frac{j\omega L_h}{1-\omega^2 L_h C_1} = \frac{j\omega L_h}{1-\left(\omega/\omega_H\right)^2}, \quad (5)$$

where $C=C_1+C_2$, the resonant frequencies can be obtained by

This article has been accepted for publication in a future issue of this journal, but has not been fully edited. Content may change prior to final publication. Citation information: DOI 10.1109/TAP.2018.2820733, IEEE Transactions on Antennas and Propagation

$$\omega_L = \frac{1}{\sqrt{L_h C}} \quad , \quad \omega_H = \frac{1}{\sqrt{L_h C_1}} \quad . \tag{6}$$

and the bandwidths by

$$BW_L = \frac{\Delta f}{f_L} = \frac{\omega_1 - \omega_2}{\omega_L} = \frac{1}{\eta}\sqrt{\frac{L_h}{C}} = \frac{1}{120\pi}\sqrt{\frac{L_h}{C}} \quad , \tag{7}$$

$$BW_H = \frac{\Delta f}{f_H} = \frac{\omega_1 - \omega_2}{\omega_H} = \frac{1}{\eta}\sqrt{\frac{L_h}{C_1}} = \frac{1}{120\pi}\sqrt{\frac{L_h}{C_1}} \quad . \tag{8}$$

Following the foregoing governing equations, the electric parameters of the MS can be designed numerically. If BW_L and BW_H are the same as those of the designed antenna, this structure can be used as a protector. By using this MS, the SAR can be decreased significantly, without influencing the electric properties of the antenna.

Generally speaking, this MS acts as a magnetic conductor when used in conjunction with antenna. Just as the structure was analyzed in reference [10], its model was set up as AMC for analysis. The protecting function of MS can be investigated as follows.

D. Verification of Antenna with Metamaterial Structure

To check the foregoing designs, a 3×3 array of the MS was investigated. The square patches array and the ground plane were printed with 35μm thick copper film on both sides of the polyimide substrate, which is with 1.0 mm thickness. From Fig. 6, it can be seen that the size of the elements, and one of the square unit cells, in terms of millimeters, are L_1=24, L_2=12, S_1=0.5, and S_2=2.5. The proposed antenna, together with the array, as shown in Fig. 8, was investigated as follows.

i) Gap (h_1)

The gap between the antenna and the MS was first checked by numerical experiment. The antenna, with the MS, was in free space. The results obtained by changing S_{11} with different gaps, are shown in Fig. 9. It was found that the antenna could not work as a dual-band when h_1=1, 2 and 3 mm. But, it started working as a dual-band when h_1=4 mm. The antenna was working well, when h_1=5, 6, 7 and 8 mm, and there was little variation in S_{11} of the antenna. But, the increase in h_1 led to higher antenna profiles. If h_1 is bigger, the whole profile of antenna with MS will become higher; if it is too small, the impact of the MS will be so great that the antenna will become much worse.

ii) On Body

With MS, the properties of the antenna must not change. Therefore, the MS on the polyimide substrate has to be researched carefully. Here, the verification was done at h_1=5mm. The antenna with MS was bent around the forearm of the human body model, Gustav. The radius of the bend was set to just 90 mm, and thus the degree of bending in the antenna and MS was not much. The antenna was placed in the middle of simulation area (FS) and the results obtained are shown in Fig. 10. The bandwidths of antenna were 2.32-2.54 GHz and 5.5-5.85 GHz in free space and 2.2-2.3 GHz and 5.4-5.8 GHz on the human body model (OB). The VSWR and input impedance are depicted in Figures 11 & 12, respectively. Apparently, the MS had little influence on the bandwidths, as well as the operation frequencies of the antenna.

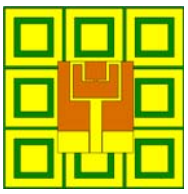

Fig. 8. Models of antenna integrated with MS.

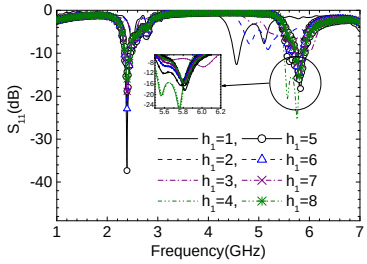

Fig. 9. Reflection coefficients obtained with different gaps (h_1) between antenna and MS.

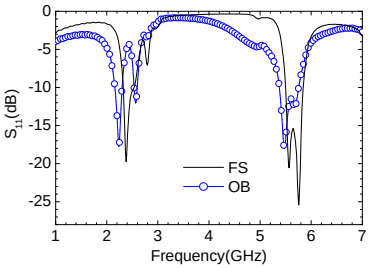

Fig. 10. Reflection coefficients of antenna with MS when the antenna was placed in the middle of simulation area (FS) and on the forearm of the human body model Gustav (OB).

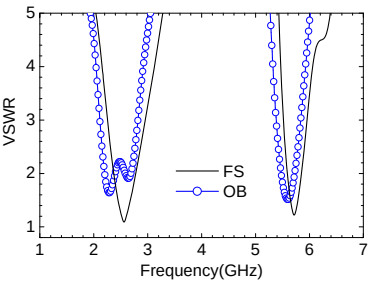

Fig. 11. VSWR of antenna with MS in the middle of simulation area (FS) and on the forearm of the human body model Gustav (OB).

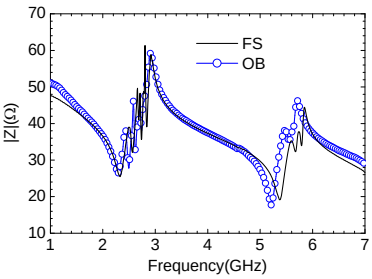

Fig. 12. Input impedance of antenna with MS in the middle of simulation area (FS) and on the forearm of the human body model Gustav (OB).

This article has been accepted for publication in a future issue of this journal, but has not been fully edited. Content may change prior to final publication. Citation information: DOI 10.1109/TAP.2018.2820733, IEEE Transactions on Antennas and Propagation

iii) SAR Reduction

The distribution of SAR values of the antenna, with the MS, is depicted in Fig. 13, when the antenna was put on the forearm of the model. The figure clearly shows reductions in SAR, implying thereby that MS can help in reducing the SAR value to the extent that the designed antenna meets the safety standards. In addition, the maximum SAR values, obtained from simulation, (see Table IV), show that they are well within the limits of the safety standards of the ICNIRP. The results thus confirm that the proposed MS in the WBAN can effectively protect the human body from electromagnetic radiation.

iv) Gain Improvement

The antenna with MS operates at a frequency of 2.32 - 2.45 GHz and 5.37 - 5.71 GHz. Radiation patterns at 2.45 GHz and 5.8 GHz were also simulated, and the respective WMS and NMS mean values of the antenna, with and without MS, are shown in Fig. 14. The results show that the back lobe of radiation patterns decreased, because of filtering of electromagnetic radiation by the MS. The maximum gain and radiation efficiency of the antenna, with and without MS, were determined and the results are presented in Table V. The gain of proposed antenna, as also of the radiation efficiency, was much more when the MS was located between the antenna and the human body model.

TABLE IV. SIMULATED SAR VALUES WHEN THE ANTENNA WAS PLACED ON HUMAN BODY (UNIT:W/KG)

Frequency(GHz)	1g	10g
2.45	2.48	0.7
5.8	3.33	0.71

TABLE V. DATA IN TERMS OF ANTENNA GAIN AND RADIATION EFFICIENCY WHEN THE ANTENNA WAS PLACED ON HUMAN BODY

Frequency (GHz)	Radiation Efficiency (%)		Gain(dB)	
	NMS	WMS	NMS	WMS
2.45	12.9	61.3	-4.1	5.2
5.80	31.5	67.2	2.33	7.7

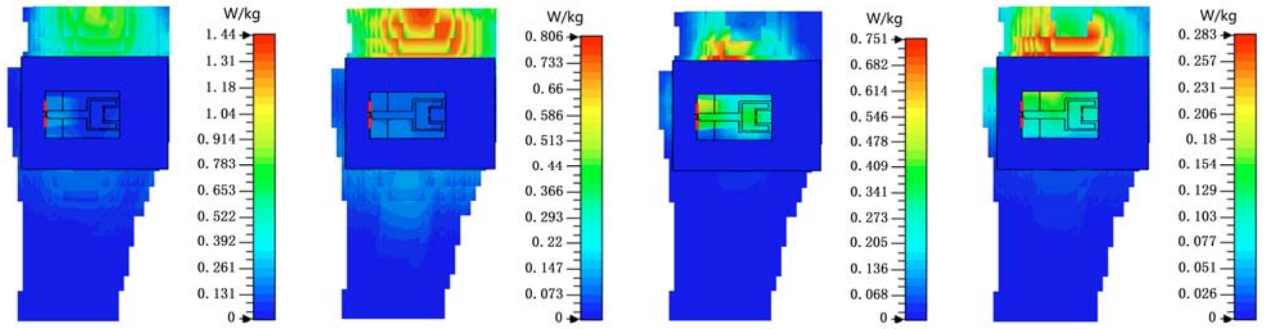

(a) (b) (c) (d)

Fig. 13. Distribution of SAR values when the antenna with MS was placed on the forearm of the Gustav model and in the simulated area: (a) and (b) at 2.45 GHz, (c) & (d) at 5.8GHz; (a) & (c) on 1g of tissue, (b) & (d) on 10g of tissue.

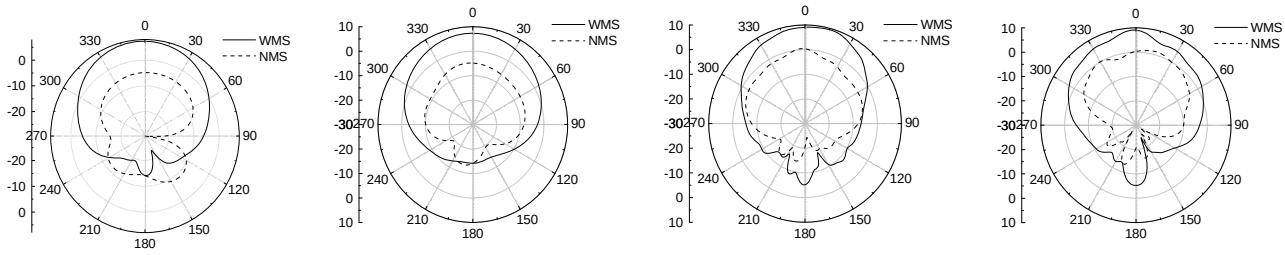

(a) (b) (c) (d)

Fig. 14. WMS and NMS mean values of the antenna, with and without MS, when the antenna was put on the forearm of the Gustav model, and in the simulated area: (a) & (b) at 2.4 GHz, (c) & (d) at 5.8 GHz; (a) & (c) E-plane, (b) & (d) H-plane.

III. ANTENNA MEASUREMENT ON REAL HUMAN BODY

The designed antenna must be experimentally validated for practical applications. The fabricated antenna was flexible and 0.15 mm thick. The SMA connector, used as a link between the antenna and the cable, was connected to the measurement device. Only the reflection coefficients in space and on real human body were measured by using vector network analyzer, Keysight N5244A (10MHz- 43.5 GHz) in the authors' laboratory. The simulated results obtained when the antenna was in a flat position, as shown in Fig. 15(a), are given in Fig. 3(b), and the measured results in Fig. 16; the operating bandwidths were 2.39-2.79 GHz and 5.66-5.92 GHz.

A. Validation of Bent Antenna

The bent antenna was placed around foam cylinders of 10mm radius, as shown in Fig. 15. In one case, the antenna was bent around x-axis (B-1), and in another, around y-axis (B-2), as shown in Fig.15 (b) and (c), respectively. Because the dielectric constant of foam is close to that of air, that is $\varepsilon_r \approx 1$, the soft sample antenna, though supported by foam cylinder, can be considered as if it was in air without affecting its substrate dielectric constant.

The experimental results obtained, in respect of S_{11}, are

This article has been accepted for publication in a future issue of this journal, but has not been fully edited. Content may change prior to final publication. Citation information: DOI 10.1109/TAP.2018.2820733, IEEE Transactions on Antennas and Propagation

(a) (b) (c)

Fig. 15. Photograph showing the shape of antenna sample when the measurements were made: when the antenna was (a) flat, (b) when it was bent around x-axis (axis of symmetry is x-axis) and (c) it was bent around y-axis bent (axis of symmetry is y-axis).

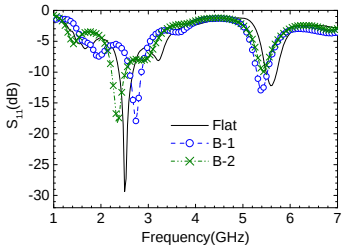

Fig. 16. Reflection coefficients of differently bent antennas; B-1relates to the antenna bent around x-axis and B-2 to the antenna bent around y-axis.

shown in Fig. 16, which obviously shows that the operating frequency shifted a little. It was interpreted earlier that the more the bend of antenna, the poorer would be its performance [20]. As the size of this flexible antenna was just 30 mm × 25 mm, it usually remains conformal to suit for the form of human body; besides, the antenna was designed to be worn by adults only. So, it was not necessary to bend the antenna beyond a certain limit.

B. Antenna investigated on Real Human Body

For the experiment in real environment, the fabricated antenna was placed on the volunteer's forearm, as shown in Fig. 17 (a). A slice of foam was inserted between the antenna and the skin, such that *d*=5 mm. The measured reflection coefficient is shown in Fig. 17 (b). It was found that the antenna was operating at 1.96-2.59 GHz and 5.38-5.71 GHz frequency bandwidths (S_{11}<-10dB), covering 2.45 GHz and 5.6 GHz frequency with wide enough band. It is worth mentioning here that this significant bandwidth was good enough. This result suggests that the effect of body tissue can be neglected.

However, this antenna cannot be directly used on human body, because its electromagnetic radiation may prove harmful when the antenna is stuck on the skin. Therefore, some measures must be taken to reduce the radiation. The following is the experiment carried out for this purpose.

C. Investigation of Antenna together with MS

To verify the functioning of the newly designed MS, a sample of 3×3 array was fabricated, and the gap between the antenna and the MS was filled with a 4 mm-thick foam layer ($\varepsilon_r \approx 1$). All the other parameters are the same as those in simulation. The antenna, together with the MS, was tested in space only and on real forearm. The testing scenario is similar to the one shown in Fig. 17 (a), and the results are depicted in

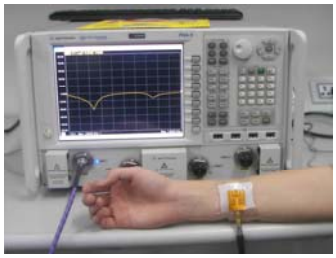

(a)

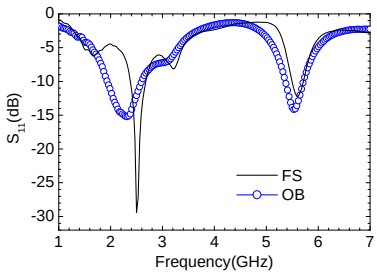

(b)

Fig. 17. Measurement results obtained when the antenna was placed on real human body and in space only: (a) Measurement scenario, (b) reflection coefficients of antenna in space only (FS) and on forearm, when d=5 mm (OB).

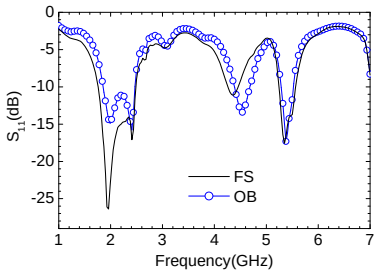

Fig. 18. Measured reflection coefficients, when the antenna with flexible MS, was in space (FS) and when on human forearm.

Fig.18. From this figure, it can be seen that the antenna operated at 1.99-2.44 GHz and 5.41-5.71 GHz. It is found that, with the MS, the frequency band offset, caused by the human body tissues, decreased. In other words, the reflection coefficient is not influenced by the human body tissues after adding MS to the antenna. The results prove that the operating frequency bands show practically no change, both in space and on body.

D. Antenna with MS on Different Human Bodies

To test the designed antenna on different human bodies, 8 volunteers, 3 male (*M*) and 5 female (*F*), and aged 21 to 36 years, were selected and designated as volunteers 1, 2, … , 8. The fabricated sample was stuck directly on the forearm of each volunteer by adhesive tape, such that d=0. The reflection coefficients were measured for all the volunteers. The results for volunteers 1 to 4 are shown in Fig. 19(a) and those for volunteers 5 to 8 in Fig. 19 (b). The bodily statistics of the volunteers, as also the bandwidths of the antenna, are presented in Table VI.

The fatness of a person is expressed by Body Mass Index (BMI), which is obtained, according to the World Health

This article has been accepted for publication in a future issue of this journal, but has not been fully edited. Content may change prior to final publication. Citation information: DOI 10.1109/TAP.2018.2820733, IEEE Transactions on Antennas and Propagation

Organization standard, by dividing a person's weight with the square of his height. Table VI shows that volunteer 1 is slightly fat and 7 a bit thin, while the others are normal. It was found that the bandwidth of antenna changed with each volunteer. The antenna could work normally at 2.4 GHz for volunteers 1, 3, 4, 5, 6 and 8, but in the case of volunteers 2 and 7, it shifted to lower operating frequency. This is because volunteer 2 is younger, while 7 is relatively thin. The fact that the reflection coefficient changed at 5.6 GHz implies that this frequency is not suitable for human body.

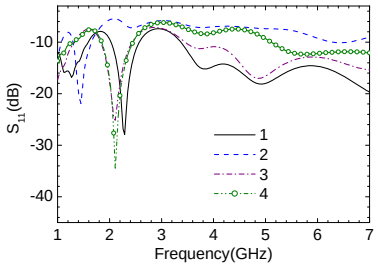

(a)

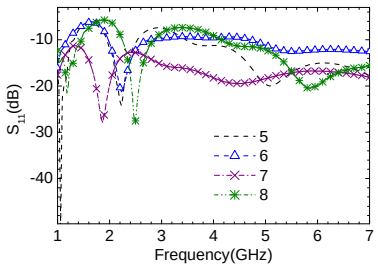

(b)

Fig. 19. Reflection coefficients when the antenna with MS touched volunteer's forearm, i.e., when d=0; reflection coefficient of (a) volunteers 1 to 4 and (b) volunteers 5 to 8.

TABLE VI. THE BODILY STATISTICS OF THE VOLUNTEERS

No.	Sex	Age	Height (cm)	Weight (kg)	BMI (kg/m^2)	Bandwidth (GHz)
1	*F*	24	163	65	26.5	2.00 -2.58
2	*M*	21	176	69	22.3	1.30 -1.65
3	*M*	23	176	70	22.6	1.82 -2.44
4	*F*	36	159	55	21.8	1.85 -2.45
5	*F*	24	156	46	18.9	1.94 -2.55
6	*F*	24	160	52	20.3	1.97 -2.77
7	*M*	24	175	55	17.8	1.24 -1.90
8	*F*	24	160	50	19.5	2.24 -2.85

IV. EXPERIMENTING ANTENNA ON BODY'S OTHER PARTS

The designed antenna with MS was tested on all the volunteers by putting it on the other parts of their bodies, such as thigh, upper arm, back and chest, as shown in Fig. 3(a). The reflection coefficients were obtained by using the vector network analyzer, Keysight N5244A (10MHz-43.5 GHz) and Star-Lab 6 (650MHz-7GHz) in the anechoic chamber of the authors' laboratory.

A. On Thigh

The reflection coefficients obtained by placing the antenna on different parts of the body, including thigh, are shown in Fig. 20. For the purpose of comparison, the simulated results obtained under similar conditions by using the human body model to check the SAR values are used here, because these values cannot be measured directly. From the figure, it can be seen that the operating bandwidths of the antenna with MS are 2.24-2.45 GHz and 5.37-5.53 GHz. In comparison with the results of the antenna on the forearm, it was found that the work frequency was offset to a higher value. This could be because, the higher amount of fat in thigh than in the forearm leads to smaller dielectric constant, resulting in higher operating frequency.

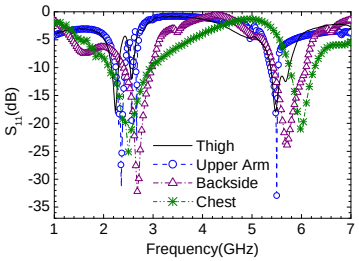

Fig. 20. The reflection coefficients obtained when the antenna, with MS, was placed on different parts of the volunteers.

The radiation patterns at 2.45 GHz and 5.8 GHz are shown in Fig. 21. These are in good agreement with simulation results. These results indicate that the simulated SAR values are reliable. Data in respect of the maximum gain and radiation efficiency of the antenna on thigh is presented in Table VII. The data includes the results obtained without the MS too. When the MS was inserted between the antenna and the human body model, the gain of the proposed antenna, as also the radiation efficiency, improved obviously.

The maximum SAR values, obtained from simulation, are shown in Table VIII; these are much lower than those stipulated by ICNIRP. In comparison to these, the SAR reductions obtained from the antenna, without the MS, are 74.6% and 86.3% at 2.45 GHz and 5.8 GHz, respectively.

B. On Upper Arm, Backside and Chest

The properties of the flexible antenna obviously improved with MS, and its SAR values are within the limits stipulated by ICNIRP. For further confirmation of the reliability of the proposed antenna, the reflection coefficients were measured by putting the antenna on the upper arm, back and chest and the results are depicted in Fig. 20. The results show that the operating frequencies changed a little as the antenna was moved between different parts of the human body. However, high frequency band offsets are obvious when the antenna was on the chest, possibly because of the higher equivalent dielectric constant of the chest.

Radiation patterns were also measured at 2.45 GHz and 5.8 GHz, when the antenna was placed on the upper arm, back and chest, and the results are shown in Fig. 21. The results indicate reduction in the back lobes and improvement in the directional

This article has been accepted for publication in a future issue of this journal, but has not been fully edited. Content may change prior to final publication. Citation information: DOI 10.1109/TAP.2018.2820733, IEEE Transactions on Antennas and Propagation

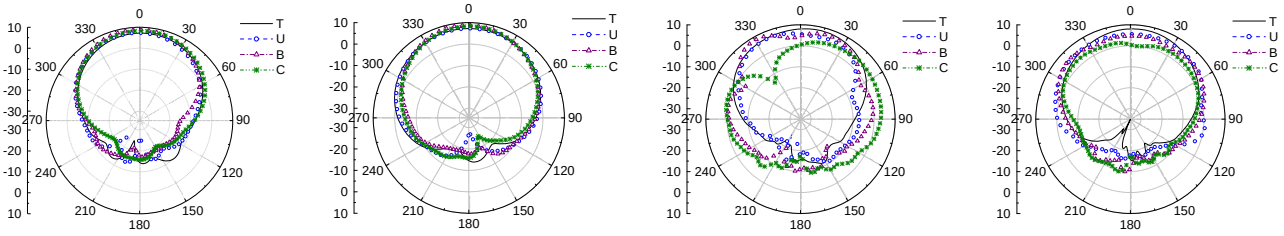

Fig. 21. Radiation patterns obtained by placing the antenna on thigh(T), upper arm(U), back (B) and chest(C): (a) & (b) at 2.4 GHz; (c) & (d) at 5.8 GHz; (a) & (c) E-plane, (b) & (d) H-plane.

TABLE VII. APPARENTLY, THE MS HAD LITTLE INFLUENCE ON THE BANDWIDTHS, AS WELL AS THE OPERATION FREQUENCIES OF THE ANTENNA.

Antenna Position	Frequency (GHz)	Radiation efficiency(%)		Gain(dB)	
		NMS	WMS	NMS	WMS
Forearm	2.45	12.9	61.3	-4.1	5.2
	5.80	31.5	67.2	2.33	7.7
Thigh	2.45	3.33	30.72	-8.18	2.15
	5.80	47.73	61.46	4.25	6.19
Upper Arm	2.45	6.4	71.04	-7.36	5.79
	5.80	29.95	75.21	1.07	5.37
Back	2.45	13.89	51.36	-2.44	6.01
	5.80	52.4	76.74	5.71	6.2
Chest	2.45	15.04	56.35	-0.75	5.83
	5.80	55.45	52.06	3.98	3.47

TABLE VIII. SIMULATED SAR VALUES, OBTAINED WITH AND WITHOUT MS, BY PLACING ANTENNA ON DIFFERENT PARTS OF HUMAN BODY MODEL (UNIT:W/KG)

Antenna Position	Frequency (GHz)	1g		10g	
		NMS	WMS	NMS	WMS
Forearm	2.45	17.50	2.48	8.99	0.7
	5.80	9.3	3.33	4.08	0.71
Thigh	2.45	16.89	4.29	5.29	1.02
	5.80	5.12	0.70	1.86	0.12
Upper Arm	2.45	11.03	2.76	4.96	0.51
	5.80	11.04	2.82	4.41	0.71
Back	2.45	8.83	2.27	3.10	0.44
	5.80	12.11	5.17	3.03	1.59
Chest	2.45	12.99	1.57	4.01	0.37
	5.80	18.95	12.44	4.12	3.89

radiation of antenna. Data in respect of the maximum gain and radiation efficiency, obtained by placing the antenna on different parts of the human body, is presented in Table VII.

Maximum SAR values were obtained from simulation of antenna, with and without the supporting MS, and the results are presented in Table VIII. These values are similar to those obtained when the antenna was placed on the forearm. The values obtained with the MS are much lower than those stipulated by ICNIRP. When the antenna with MS was put on the upper arm, the SAR reductions are 75% and 74.5%, at 2.45 GHz and 5.8 GHz, respectively, compared to those obtained without the supporting MS. On other parts of the human body, results, similar to those in Table VIII, can be obtained.

V. CONCLUSION

This paper demonstrates and confirms experimentally that the proposed dual-band antenna, integrated with MS, is suitable for WBAN applications. By printing the antenna and the MS on polyimide substrate, very good properties were obtained. The proposed antenna is flexible, thin and tiny; it can be moved easily between different parts of the human body. When the antenna was supported by MS, not only the gain of antenna increased, its SAR value also decreased significantly in operating frequency bands of 2.32-2.45 GHz and 5.37-5.71 GHz.

The safety of the proposed antenna, with MS, was investigated for application on human bodies. The antenna was tested by placing it on the forearm, thigh, upper arm, back and chest of a real human body, and on different human bodies. The results obtained are in good agreement with those obtained by simulation, using CST software. The performances of the antenna on the upper arm and thigh are similar. When the antenna was placed on the back and chest, its operating frequency increased, because of the viscera. When the antenna was used with MS, the SAR values decreased by more than 70%, which is very much within the limits stipulated by ICNIRP. To the best of the authors' knowledge, this is the first time that someone comes up with a flexible dual-band antenna with MS, and tests its performance by simulation and measurement on different parts of a real human body and on different human bodies of both men and women. In addition, the polyimide substrate used in the proposed antenna, makes the fabrication easy and inexpensive. Besides, its light weight and softness, together with the way it fits to different parts of the human body, render the antenna easily wearable. Implanting antenna in the human body must be the next step of development in this field.

REFERENCES

[1] S. N. Ramli, R. Ahmad, M. F. Abdollah et al. "A biometric-based security for data authentication in wireless body area network (WBAN)," in *Proc. Int. Adv. Communicat. Technology Symp.*, 2013, pp. 998-1001.

[2] M. Hirvonen, C. Böhme, D. Severac et al. "On-body propagation performance with textile antennas at 867 MHz," *IEEE Trans. Antennas Propagat.*, vol. AP-61, no. 4, pp. 2195-2199, April 2013.

[3] W. Lei, H. Chu and Y. X. Guo. "Design of a circularly polarized ground radiation antenna for biomedical applications," *IEEE Trans. Antennas Propagat.*, vol. AP-64, no. 6, pp. 2535-2540, June 2016.

[4] H. R. Khaleel, H. M. Al-Rizzo, D. G. Rucker et al. "A compact polyimide-based UWB antenna for flexible electronics," *IEEE Antennas Wireless Propagat. Lett.*, vol. 11, pp. 564-567, 2012.

[5] D. Unnikrishnan, D. Kaddour, S. Tedjini et al. "CPW-fed inkjet printed UWB antenna on ABS-PC for integration in molded interconnect devices

technology," *IEEE Antennas Wireless Propagat. Lett.*, vol. 14, pp. 1125-1128, 2015.
[6] K. Hettak, T. Ross, R. James, et al. "Flexible polyethylene terephthalate-based inkjet printed CPW-fed monopole antenna for 60 GHz ISM applications," in *Proc. Microwave Integrated Circuits Symp.*, 2013, pp. 476-479.
[7] N. A. Elias, N. A. Samsuri, M. K. A. Rahim, et al. "Effects of human body and antenna orientation on dipole textile antenna performance and SAR," in *Proc IEEE APCAE, Symp*., 2012, pp. 132-136.
[8] N. A. L. Alias, N. A. M. Affendi, Z. Awang, et al. "Preliminary studies on the use of natural rubber in the design of flexible microstrip Antennas," in *Proc.IEEE Microwave Symp.*, 2013, pp. 454-459.
[9] B. S. Cook and A. Shamim. "Utilizing wideband AMC structures for high-gain inkjet-printed antennas on lossy paper substrate," *IEEE Antenna Propagat. Lett.*, vol. 12, pp. 76-79, 2013.
[10] P. Prakash, M. P. Abegaonkar, A. Basu et al. "Gain enhancement of a CPW-fed monopole antenna using polarization-insensitive AMC structure," *IEEE Antennas Wireless Propagat. Lett*., vol. 12, pp. 1315-1318, 2013.
[11] S. Zhu and R. Langley. "Dual-band wearable textile antenna on an EBG substrate," *IEEE Trans Antennas Propagat.*, vol. AP-57, no. 4, pp. 926-935, April, 2009.
[12] Y. H. Di, X. Y. Liu and M. M. Tentzeris. "A conformable dual-band antenna equipped with AMC for WBAN applications," in *Proc. Asia-Pacific Antennas Propagat. Symp.*, 2014, pp. 388-391.
[13] IEEE. *Standard for safety levels with respect to human exposure to radio frequency electromagnetic fields*, 3 kHz to 300 GHz c95.1a-1998. EU: Institute of Electrical and Electronics, 1999.
[14] H. R. Raad, A. I. Abbosh, H. M. Al-Rizzo et al. "Flexible and compact AMC based antenna for telemedicine applications," *IEEE Trans. Antennas Propagat.*, vol. AP-61, no. 2, pp. 524-531, Feb. 2013.
[15] CST Microwave Studio. Computer Simulation Technology, Framingham, MA, 2016[Online]. Available: http://ww.cst.com
[16] M. P. David, *Microwave engineering*, third edition, USA, 2005.
[17] H. Vladimír, "Planar antenna in proximity of human body models," in *Proc. European Conf. Antennas Propagat. Symp.*, 2013, pp. 3309-3311.
[18] Q. Liu, Y. Xi, A. C. F. Reniers et al. "Analysis of the reflection characteristics of a planar EBG structure on lossy silicon substrates," in *Proc. European Antennas Propagat. Symp.,* 2016, pp. 1-4.
[19] Y. Li, K. Esselle, A. Weily, et al. "A dual-band planar compact artificial magnetic conductor," in *IEEE AP-S, Symp.,* 2005, vol. 4B, pp. 451-454.
[20] J. Liu, F. Dai, Y. Zhang, et al. "Bending effects on a flexible yagi-uda antenna for wireless body area network," in *Proc.IEEE APEMC Symp.*, 2016, pp. 1001-1003.

Mengjun Wang was born in Hebei, China, in 1978. He received his B.S. degree in information engineering and M.S. degree in physical electronics from Hebei University of Technology, Tianjin China, in 1999 and 2005, respectively, and Ph.D. degree from Tianjin University, Tianjin, China, in 2008.

He is working as an associate professor at School of Electronics and Information Engineering, Hebei University of Technology, Tianjin, China. His research interests include microwave radio frequency technology, flexible electronics devices and electromagnetic compatibility.

Ze Yang was born in Hebei, China, in 1991. She received her B.S. degree from Hebei University of Technology, Langfang Branch, Hebei, China, in 2016, and is currently working for Master's degree in communication and information system at Hebei University of Technology, Tianjin, China.

Her research interests include flexible antenna and electromagnetic compatibility.

Jianfei Wu was born in Jiangsu, China, in 1983. He received his M.S. degree in electrical engineering in 2008 and Ph.D. degree in information and communication engineering from National University of Defense Technology, Changsha, China, in 2013.

He is currently a lecturer, carrying out postdoctoral research in National University of Defense Technology. He worked for two years (2010-2012) on a China Scholarship at National Institute of Applied Sciences (INSA Toulouse, France) as a visiting Ph.D. student. His current research interests include EMC testing, modeling and simulation of IC circuits.

Jianhui Bao was born in Heilongjiang province, China, in 1987. She received her B.S. degree in electronic engineering and Ph.D. degree in electronic field and microwave technology from Xidian University in 2010 and 2016, respectively.

She is now working as a lecturer at School of Electronics and Information Engineering, Hebei University of Technology, Tianjin, China. Her research interests include flexible electronic devices, millimeter wave antenna and antenna array.

Jianying Liu was born in Tianjin, China, in 1991. She received her B.S. degree from Tianjin University of Technology, Tianjin, China, in 2014. She is currently working for her Master's degree in communication and information system at Hebei University of Technology, Tianjin, China.

Her research interests include flexible antenna and electromagnetic compatibility.

Lulu Cai was born in Hebei, China, in 1992. She received her B.S. degree from Hebei University, Hebei, China, in 2015, and is currently working for Master's degree in communication and information system at Hebei University of Technology, Tianjin, China.

Her research interests include flexible antenna and electromagnetic compatibility.

Tao Dang received his B.S. and M. S. degrees in electronics engineering from Northwestern Polytechnical University, Xi'an, Shaanxi, China, in 2002, and from Civil Aviation University of China, Tianjin, in 2005, respectively. Now he is working for PhD degree in electronics engineering at Airforce Engineering University, Xi'an, Shaanxi, China.

He is now working as a senior engineer at Sichuan Jiuzhou Electronic Technology Co., Ltd, Mianyang, Sichuan, China. His research interests include microwave technology and antenna design.

Hongxing Zheng (M'01) received his Ph.D. degree in electronic engineering from Xidian University, Xi'an, in 2002. He is currently a Professor at School of Electronics and Information Engineering, Hebei University of Technology, Tianjin, China. He has authored six books and book chapters and more than 200 journal papers and 100 conference papers. He holds 40 China patents, issued in 2017. His recent research interests include wireless communication, design of microwave circuit and antenna, and computational electromagnetics.

Dr. Zheng is a Senior Member of the Chinese Institute of Electronics (CIE). He received the Young Scientists Award, in 2008, presented by the Tianjin Municipality, China. He is listed in *Who's Who in the World* and in *Who's Who in the Science and Engineering in the World.*

Erping Li (S'91–M'92–SM'01–F'08) received his Ph.D. degree in electrical engineering from Sheffield Hallam University, Sheffield, U.K., in 1992. From 1993 to 1999, he was a Senior Research Fellow, Principal Research Engineer, Associate Professor, and Technical Director at Singapore Research Institute and Industry. In 2000, he joined the Singapore National Research Institute of High Performance Computing as the Principal Scientist and the Director of the Department of the Electronic and Photonics. He also holds the post of Distinguished Professor at Zhejiang University. He authored or coauthored more than 400 papers, published in various conference proceedings and reputed international journals. He authored two books also. His research interests include electrical modeling and design of micro/nano-scale integrated circuits, 3-D electronic package integration, and nano-plasmonic technology.

Dr. Li is a Fellow of the MIT Electromagnetics Academy, USA. He received numerous awards, including the IEEE Electromagnetic Compatibility (EMC) Richard Stoddard Award for outstanding performance. He has served as an Associate Editor for a number of IEEE TRANSACTIONS AND LETTERS. He has served as a General Chair and Technical Chair, for many international conferences. He was the founding General Chair for Asia-Pacific EMC Symposium in 2008, 2010, and 2012. He has been invited to deliver talks and plenary speeches at various international conferences and forums.